

Ni/Bi bilayers: The effect of thickness on the superconducting properties

Gabriel Sant'ana ^{*}, David Möckli, Alexandre da Cas Viegas, Paulo Pureur and Milton A. Tumelero [†]

Instituto de Física, Universidade Federal do Rio Grande do Sul, 91501-970 Porto Alegre, Brazil

Abstract

Nickel/Bismuth (Ni/Bi) bilayers have recently attracted attention due to the occurrence of time-reversal symmetry breaking in the superconducting state. Here, we report on the structural, magnetic and electric characterization of thin film Ni/Bi bilayers with several Bi thicknesses. We observed the formation of a complex layered structure depending on the Bi thickness caused by the inter-diffusion of Bi and Ni which leads to the stabilization of NiBi₃ at the Bi/Ni interface. The superconducting transition temperature and the transition width are highly dependent on the Bi thickness and the layer structure. Magnetoelectric transport measurements in perpendicular and parallel magnetic fields were used to investigate the temperature-dependent upper critical field within the framework of the anisotropic Ginzburg-Landau theory and the Werthamer–Helfand–Hohenberg model. For thicker samples, we observed a conventional behavior, similar to that shown by NiBi₃ bulk samples, including a small Maki parameter ($\alpha_M = 0$), no spin-orbit scattering ($\lambda_{SO} = 0$) and nearly isotropic coherence length ($\gamma = \xi_{\perp}(0)/\xi_{\parallel}(0) \approx 1$). The values obtained for these properties are close to those characterizing NiBi₃ single crystals. On the other hand, in very thin samples the Maki parameter increases to about $\alpha_M = 2.8$. In addition, the coherence length becomes anisotropic ($\gamma = 0.32$) and spin-orbit scattering ($\lambda_{SO} = 1.2$) must be taken into account. Our results unequivocally show that the properties characterizing the superconducting state in the Ni/Bi are strongly dependent on the sample thickness.

Keywords: Ni/Bi bilayer, NiBi₃ compound; spin-orbit superconductors; unconventional superconductivity

^{*}gabriel.santana.dasilva@outlook.com

[†]matumelero@if.ufrgs.br

1 Introduction

Time reversal symmetry-breaking (TRSB) in the superconducting state has been a strongly discussed topic in condensed matter physics. Superconductors showing TRSB have been considered as a great promise for technological advancements in quantum computing and spintronics, as they are expected to exhibit Majorana edge modes [1, 2] and spin-triplet pairing [3]. Currently, this phenomenon has been observed in uranium-based heavy fermions and in the perovskite Sr_2RuO_4 [4, 5, 6]. However, the occurrence of spontaneous TRSB superconductors in non-centrosymmetric 2D systems had not been reported until Gong *et al.* observed this property in nickel/bismuth (Ni/Bi) bilayers [7].

Interestingly, while Ni does not exhibit superconductivity (SC) and Bi only displays this property below 0.5 mK at ambient pressure [8], a superconducting transition with a critical temperature (T_c) of approximately 4 K occurs when both elements are grown as a Ni/Bi thin film bilayer. This heterostructure was initially investigated by Moodera *et al.* [9] and LeClair *et al.* [10], who used tunneling measurements to suggest that SC potentially occurs across the entire bilayer. Similar conclusions were later reported in the experimental studies of Gong *et al.* [7] and Chauhan *et al.* [11], the latter arguing in favor of a p -wave nature of symmetry pairing. Other experimental works have observed signatures of unconventional SC consistent with chiral p -wave behavior [12, 13].

Although many studies consider the Ni/Bi bilayer as a potential unconventional superconductor, the presence of a NiBi_3 layer formed at the interface may be an alternative explanation for the observed phenomenology. This particular intermetallic compound is described as a strong coupling s -wave superconductor with T_c around 4.1 K [14, 15, 16], essentially the same T_c as for the Ni/Bi bilayer heterostructure. Regardless of the preparation technique, spontaneous formation of NiBi_3 is observed when the deposition temperature of the bilayer is higher than 110K [17, 18, 19]. However, when the Ni/Bi bilayer is prepared at 4.2 K, to avoid interdiffusion, Liu *et al.* [19] verified that neither NiBi_3 is formed nor the resulting bilayer is superconducting.

In essence, the presence of an interfacial NiBi_3 layer appears to be a necessary condition for the observation of a superconducting transition in the Ni/Bi bilayer. A theoretical model proposed by Chao considers the presence of NiBi_3 acting as a mechanism to induce SC in the Bi layer via the proximity effect [20]. In addition, the model takes into account the strong spin-orbit interaction related to Bi and the exchange coupling coming from Ni to provide a reasonable explanation for the p -wave-like Andreev reflection signatures seen previously [12]. In other words, the model proposes a chiral p -wave symmetry with non-trivial topological phase to describe the superconducting state in the Bi/Ni bilayer system. Therefore, at this point, it seems unclear whether the SC in Bi/Ni originates directly from NiBi_3 at the interface or whether it is induced by the proximity effect in the adjacent Bi layer. It is nonetheless unclear if these configurations host an unconventional

superconducting state.

To further contribute, we study the layered Bi/Ni system with its superconducting properties including: critical temperature, upper critical field, and coherence length as functions of the Bi layer thickness. Our analyses are based on Ginzburg-Landau and Werthamer–Helfand–Hohenberg (WHH) models, considering two different magnetic field configurations: parallel (aligned with the current) and perpendicular (out of the film plane). Our findings suggest the presence of a thickness-dependent crossover point at which unconventional properties potentially emerge.

2 Experimental details

We grew Ni/Bi bilayer thin films on silicon oxide (100 nm) covered silicon wafer substrates by using the magnetron sputtering deposition technique. The substrates were kept at room temperature. We prepared several samples with a fixed 8 nm layer of Ni and layers of Bi with thicknesses ranging from 10 to 80 nm. The purity of both Ni and Bi targets was 99.99% and the power employed for the depositions was 65 W (RF) for the Ni target and 10 W (DC) for the Bi target. A capping Ti layer of 2 nm was applied to all samples to prevent oxidation. The vacuum chamber base pressure was maintained at 2×10^{-7} Torr, and the deposition working pressure was set to 1×10^{-3} Torr by using 200 sccm flux of ultrapure argon gas (99.9999%).

Rutherford backscattering spectroscopy (RBS) using 1.5 MeV He⁺ beam was employed to determine the samples' thicknesses. To study the crystallographic properties we applied X-ray diffraction (XRD) in the $\Theta - 2\Theta$ configuration with Cu α 1 radiation. Magnetization was measured as a function of the field at room temperature in a VSM EV9 magnetometer manufactured by Microsense Inc.

For the magneto-electrical measurements, we implemented a standard four-probe method where the in-plane current was applied at the extremities of the sample, while two inner contacts were used to measure the longitudinal voltage drop. In this arrangement, two magnetic field configurations were used: (i) parallel, with the field applied along the current direction, and (ii) perpendicular to the substrate plane. The magneto-transport experiments were performed using a set-up based on a CMag9 cryocooler manufactured by Cryomagnetics Inc.

3 Results and Discussion

3.1 Structural and magnetic characterization

Fig. 1a displays the XRD patterns obtained for Ni(8nm)/Bi(x) samples with $x = 10$, 30 and 60 nm. The presence of NiBi₃ peaks is evident, while no peaks of individual Bi

and Ni layers were observed. This result is in agreement with previous reports that also notice the formation of the inter-metallic NiBi_3 compound [17, 19, 18]. The XRD pattern is consistent with the orthorhombic structure of NiBi_3 with $Pnma$ space group. We did not observe the NiBi compound in our samples, which contrasts with a previous study [19].

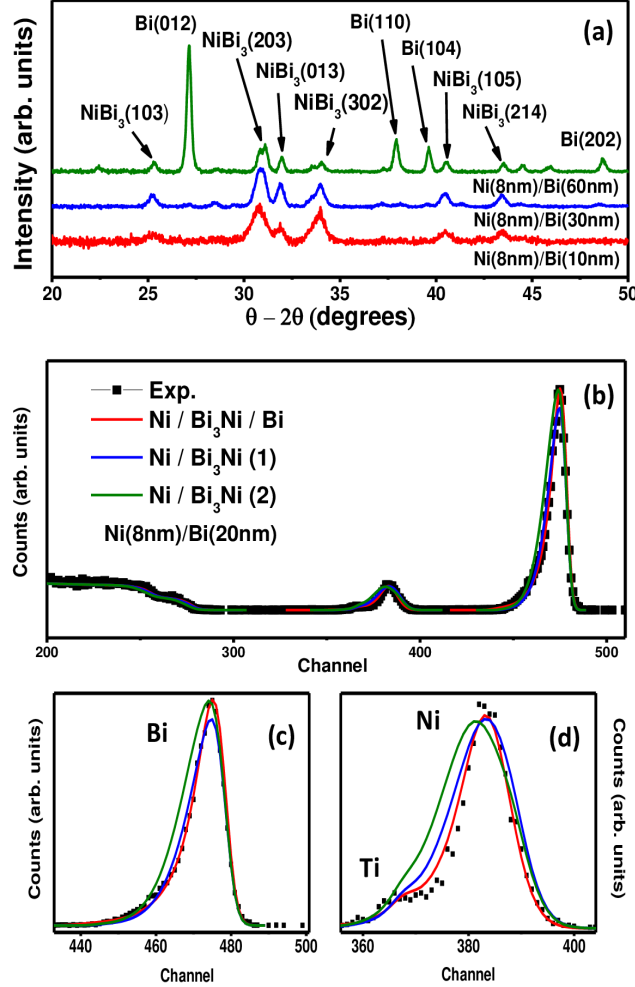


Figure 1: (a) The XRD pattern of $\text{Ni}(8\text{nm})/\text{Bi}(x)$, for $x = 10$ nm (red), $x = 30$ nm (blue) and $x = 60$ nm (green). (b) The RBS spectra for $\text{Ni}(8\text{nm})/\text{Bi}(20\text{nm})$ with close-ups for the (c) Bi and (d) Ni and Ti peaks. The green and blue lines in panels (c) and (d) correspond to different SIMNRA simulations for a NiBi_3/Ni bilayer, while the red line is a simulation for a $\text{Ni}/\text{NiBi}_3/\text{Bi}$ trilayer.

Additional information on the structural properties was obtained from Gaussian fitting the XRD peaks in Fig. 1a. The full-width at half maxima (FWHM) decreases with growing sample thickness, indicating that thicker samples are more crystalline. In the $\text{Ni}(8\text{nm})/\text{Bi}(60\text{nm})$ sample (shown in green), the observed pure Bi peaks (012), (110), (104), and (202) are consistent with the $R\bar{3}m$ trigonal structure. The presence of solid Bi suggests a limit in the formation of NiBi_3 , which can be interpreted based on two contributions: (i) A diffusive limited process, in which the Bi diffuses into the Ni layer

forming the NiBi_3 layer; (ii) A kinetic limited process, in which the Bi reacts with Ni forming the NiBi_3 layer until one of the layers (Bi or Ni) is fully consumed.

Fig. 1b presents the RBS spectrum obtained for the $\text{Ni}(8\text{nm})/\text{Bi}(20\text{nm})$ sample, whereas Figs. 1c,d provide zoomed-in views of the Bi and Ni peaks, respectively. The capping Ti layer is also detected as a shoulder in Fig. 1d. To determine the sample stoichiometry and thickness, we utilized the SIMNRA software and the values of bulk mass density. In Figs. 1c,d, the green and blue lines correspond to simulations of a Ni/NiBi_3 bilayer with: (1) focus on simulating the maxima of the Ni peak; and (2) focus on simulating the maxima of the Bi peak, whereas the red line corresponds to the simulation of the trilayer $\text{Ni}/\text{NiBi}_3/\text{Bi}$. The latter offers the best fit for the experimental data. This suggests that even for the bilayer with the lowest Bi thickness, a thin layer of Bi remains after the formation of NiBi_3 at the interface. Consequently, this observation can be assumed as evidence in favor of the diffusive limited NiBi_3 formation process. Additionally, the RBS simulation for the $\text{Ni}(8\text{nm})/\text{Bi}(20\text{nm})$ indicates a thickness of 11 nm for Bi, 18 nm for NiBi_3 and 7 nm for Ni, approximately. This means that the relative consumption rate between Ni and Bi is close to (1:9) nm, which agrees with the findings of Vaughan *et. al* [18], who makes use of a polarized neutron scattering technique.

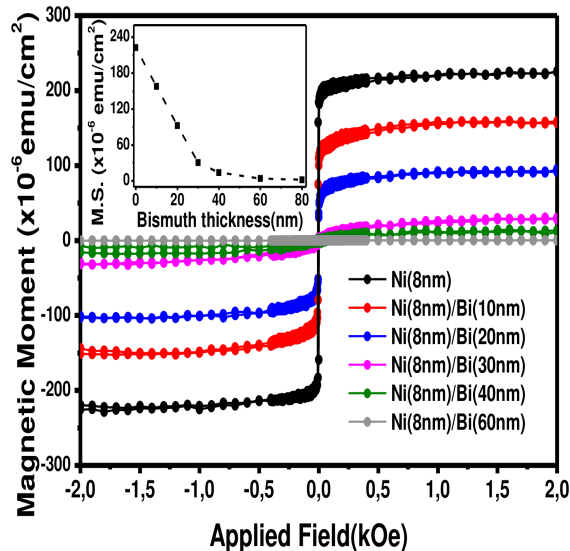


Figure 2: Magnetic moment normalized by the area of each sample. Measurements were made at room temperature as functions of the in-plane magnetic field. Inset: magnetic moment of saturation (M.S.) normalized by area vs bismuth thickness.

Fig. 2 shows the magnetic moment normalized by the sample's area as a function of the in-plane applied magnetic field. These experiments were carried out at room temperature. Previous studies have not reported any magnetic order in NiBi_3 [21, 22]. Therefore, we assume that the magnetic moment observed in our samples originates from the Ni layer. Results in Fig. 2 indicate that the presence of the Bi layer with increasing thickness gradually suppresses the Ni magnetic moment. The inset in Fig. 2 depicts the magnetic

moment of saturation (M.S.) for different Bi thicknesses. Clearly, the M.S. vanishes for samples where the Bi layers have a thickness larger than 40 nm. The formation of the NiBi₃ compound at the interface of the bilayers is probably the most important effect leading to the progressive suppression of ferromagnetism.

We estimated the thickness of the ferromagnetic portion of the Ni layer by assuming the bulk magnetization and structural parameters. Interestingly, for an 8 nm pure Ni layer (black dots in Fig. 2) the estimation yielded an effective ferromagnetic Ni layer thickness of about 4.8 nm. This suggests the occurrence of magnetically dead Ni sub-layers within the thin film structure. Such an interpretation was previously proposed by Liebermann *et. al* to account for similar observations in Ni thin films at room temperature [23]. In our case, the dead layers might be related to the oxidation of Ni close to the interface with the SiO₂ substrate. Regarding the Ni/Bi bilayers, we estimate thicknesses for the ferromagnetic Ni of 3.4 nm, 2.1 nm, and 0.8 nm for Ni(8nm)/Bi(x) with $x = 10, 20$ and 30 nm, respectively. These results indicate a consistent consumption rate close to (1:9) nm, similar to the one obtained from the RBS analysis.

Based on the characterization, we are led to the conclusion that two distinct types of Ni/Bi layered structures are present in our bilayers. For Bi depositions up to 30 nm, we effectively obtained a Ni/NiBi₃/Bi trilayer, resembling a heterostructure configuration of metal/superconductor/ferromagnet. In contrast, Bi thicknesses exceeding 30 nm reveal the occurrence of a progressive suppression of ferromagnetism in the Ni film, so that the samples behave as a NiBi₃/Bi bilayer, which is akin to a metal/superconductor system. Here, we consider that the Bi layer behaves as a metallic component, which is expected due to its low thickness [24].

3.2 Thickness-dependence of the critical temperature

Fig. 3a shows the normalized resistance (R/R_{5K}) vs. temperature, while Fig. 3b displays T_c as a function of the Bi thickness. Since our lowest reachable temperature is 1.8 K, we define T_c as the temperature where the measured resistance decreases to 90% of the normal state resistance. Similar profiles of T_c vs. thickness were reported in Refs. [7, 12, 18, 19] for Ni/Bi bilayers. For samples deposited with higher Bi thickness, i.e. Ni(8nm)/Bi(40nm), Ni(8nm)/Bi(60nm) and Ni(8nm)/Bi(80nm), the superconducting transition is sharp and has a $T_c \approx 4.05K$, similar to those reported for the NiBi₃ compound (red dashed-line on Fig. 3b). On the other hand, a large broadening in the superconducting transition is observed for the samples Ni(8nm)/Bi(20nm) and Ni(8nm)/Bi(30nm). The transition for the sample Ni(8nm)/Bi(10nm) was not observed to occur in the measured temperature range. The broadening of the superconducting transition is usually related to the disorder. We have indeed observed some increase in lattice disorder by looking at the FWHM in the XRD patterns for samples with small

Bi thicknesses. Nonetheless, we would like to point out that the transition widens quite significantly when the Bi thickness is reduced below the 40 nm threshold. For instance, the transition broadening in the Ni(8nm)/Bi(30nm) sample is about 10 times larger than that in the Ni(8nm)/Bi(40nm) specimen. The FWHM, however, changes much more slowly in the same range of Bi thickness. Therefore, we believe that the broad transition might be related to other effects apart from lattice disorder.

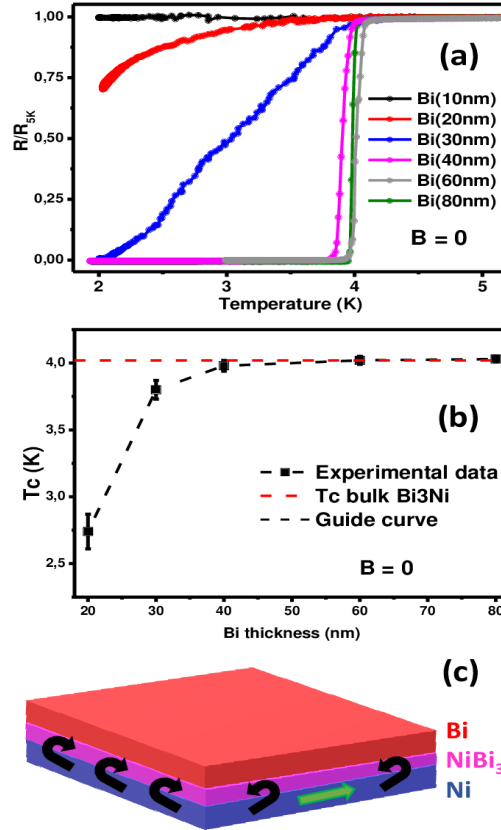


Figure 3: (a) Normalized resistance as a function of temperature for Ni(8nm)/Bi(x) samples. (b) T_c as a function of Bi thickness. (c) Schematic illustration of the Ni/Bi₃Ni/Bi trilayer. The black arrows indicate the stray field originating from the Ni layer and green arrow corresponds to the in-plane magnetization.

By comparing the T_c curve in Fig. 3b with the inset in Fig. 2, we observe that a strong widening of the superconducting transition occurs in samples with a non-zero magnetic moment. This leads us to speculate that the remaining ferromagnetic Ni layer generates a highly non-uniform magnetic stray field, as depicted in Figure 3c. This stray field acts on the NiBi₃ layer and causes a significant detrimental effect on the superconducting state of the bilayers, particularly for the samples with thinner superconducting layers, resulting in the sharp reduction of the T_c . The influence of stray fields in Ni/Bi bilayers has been discussed in a previous study [25].

The primary factor contributing to the broadening of the red and blue transition curves in Fig. 3a probably comes from the stray field generated by the nearby ferro-

magnetic Ni. Although less likely, there might be another contribution to this effect: a crossover from a three-dimensional (3D) to a two-dimensional (2D) behavior. This is expected to occur when the thickness of the superconducting layer becomes comparable to or smaller than the coherent length. The change in dimensionality induces significant fluctuations in the order parameter due to the influence of interface and surface scattering, resulting in a strong decrease of the critical temperature [26], similar to that shown in Fig. 3b. We will return to this point later in this manuscript.

3.3 Superconducting properties

In Fig. 4 we show the normalized resistance vs. temperature results measured at different magnetic fields for two field orientations, namely, perpendicular to the plane of the film (a-c) and parallel (d-f) to the electrical current. Applied fields are from 1-5 kOe in steps of one (colors varying from red to gray), and 1-8 kOe (colors varying from red to purple) for parallel and perpendicular field directions, respectively. Corrections for the demagnetizing effects are negligible in all cases. Increasing fields move the transition $T_c(B)$ towards lower temperatures as expected. Nevertheless, the width of the transition seems to increase much faster in samples with low Bi thickness, which can also be related to the stray field generated by the ferromagnetic Ni layer. From Fig. 4, we extract the upper critical field $B_{c2,\perp}$ and $B_{c2,\parallel}$ as a function of the reduced temperature $t = T/T_c$. The obtained experimental points are shown in Fig. 5.

In the case of perpendicular magnetic fields the transition from the normal state to the superconducting vortex phase is described by the linear temperature dependence shown by the red points in Fig. 5a-c for all samples. Assuming that the orbital effect is the dominant limiting mechanism introduced by the applied magnetic field, we estimate the in-plane zero-temperature coherence length $\xi_{\parallel}(0)$ by fitting the red experimental data to the following expression from the anisotropic Ginzburg-Landau (AGL) model [27]:

$$B_{c2,\perp}(t) = \frac{\Phi_0}{2\pi\xi_{\parallel}^2(0)}(1-t), \quad (1)$$

where Φ_0 is the flux quantum. The extracted values for $\xi_{\parallel}(0)$ are listed in Tab. 1. The values of $\xi_{\parallel}(0)$ are close to those reported by Vaughen [18] for a Ni/Bi bilayer of about 13.8 nm and slightly lower than those for a NiBi₃ single crystal [15], where $\xi_a(0) = 18.1$ nm and $\xi_c(0) = 14.3$ nm along crystalline a and c axis, respectively. Another relevant result is the weak dependence of $\xi_{\parallel}(0)$ with respect to the Bi thickness. Here, one would expect a reduction of $\xi_{\parallel}(0)$ (bulk-like) with the reduction of thickness [28], once thinner samples should present higher levels of disorder, as indeed shown by the residual resistivity ratio (RRR) also displayed in Tab. 1. Consequently, we are lead to consider that disorder does not play a significant role in the properties of the superconducting state of our samples,

at least those directly dependent on the coherence length.

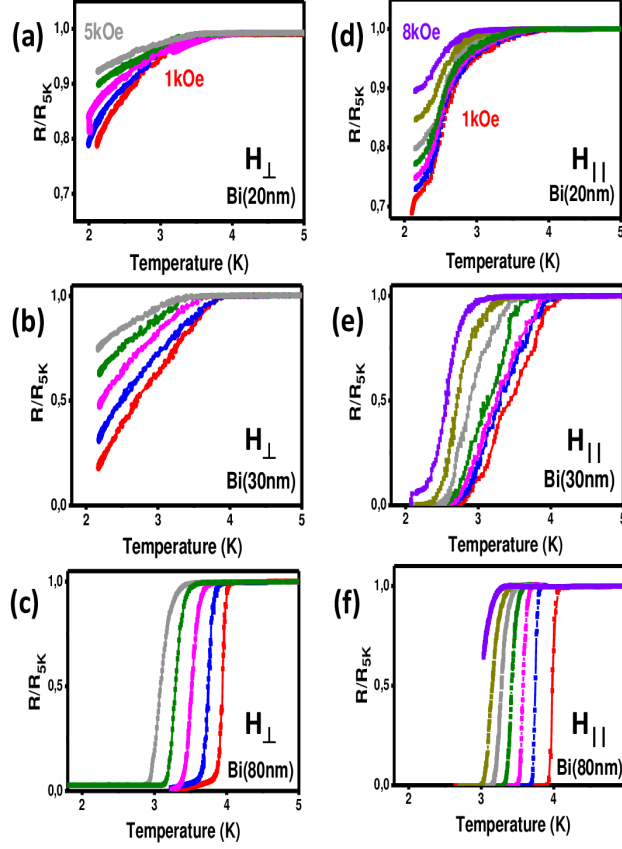


Figure 4: Normalized resistance in 5 K vs. temperature for perpendicular (a-c) and parallel (d-f) applied magnetic field orientation for Ni(8nm)/Bi(x) samples with $x = 20, 30$ and 80 nm. The colors start from 1 kOe (red) up to 5 kOe (gray) for perpendicular and up to 8 kOe (purple) for parallel magnetic fields.

The experimental data corresponding to in-plane magnetic fields are represented by the black points in Fig. 5a-c. We fitted these results to the the 3D AGL model [27], which predicts the that the upper critical field for in-plane direction is given by

$$B_{c2,\parallel} = \frac{1.69\Phi_0}{2\pi\xi_{\parallel}(0)\xi_{\perp}(0)} (1 - t), \quad (2)$$

where the out-of-plane coherence length (ξ_{\perp}) is introduced by assuming the effective mass anisotropy approximation. By fitting the in-plane field data with the above expression (black line on Fig. 5a-c) we extracted the values of $\xi_{\perp}(0)$, which are also listed in Tab. 1.

For samples with 30 nm and 80 nm of Bi, the anisotropy factor defined as $\gamma = \xi_{\perp}(0)/\xi_{\parallel}(0)$ is close to 1, indicating an isotropic behavior similar to the bulk NiBi₃ type-II superconductor. On the other hand for the Ni(8nm)/Bi(20nm) specimen, the $\xi_{\perp}(0)$ is smaller than $\xi_{\parallel}(0)$, revealing the occurrence of an anisotropy in the coherence length that

is characterized by the $\gamma = 0.3$. At first glance, one might consider that the reduction in $\xi_{\perp}(0)$ would be related to 2D effects due to the reduction of the NiBi₃ thickness. However, the 2D GL theory predicts that $B_{c2,\parallel}$ varies with temperature as $\sim (1 - t)^{1/2}$ [29], which does not fit to our data.

Table 1: Extracted coherence lengths within the framework of anisotropic Ginzburg-Landau theory, anisotropy factor γ and residual resistivity ratio.

Sample	$\xi_{\parallel}(0)$ (nm)	$\xi_{\perp}(0)$ (nm)	$\gamma = \xi_{\perp}/\xi_{\parallel}$	RRR
Ni(8nm)/Bi(20nm)	13.3 ± 0.4	4.2 ± 0.4	0.3	1.7
Ni(8nm)/Bi(30nm)	13.1 ± 0.2	15.1 ± 0.6	1.2	1.8
Ni(8nm)/Bi(80nm)	11.1 ± 0.3	14.5 ± 0.3	1.3	3.1

Another possibility is the effect of a dimensional crossover. The enhancement of $B_{c2,\parallel}$ provoked by the 3D-2D dimensional crossover usually occurs below a characteristic temperature known as T^* [26, 27, 30, 31]. In our case, however, the linear temperature dependence shown by the experimental data clearly implies the validity of the $T^* < T < T_c$ regime. For this reason, the parallel upper critical field should approach the 3D value of the ordinary type-II superconducting phase. Based on these arguments, we speculate that the reduction of $\xi_{\perp}(0)$ in thin samples may be related to an effect other than disorder and dimensional crossover.

The Ni/Bi system has been widely investigated due to the possibility of hosting unconventional superconductivity, where the spin-orbit coupling is supposed to play a key role. Assuming that the superconductivity in our bilayers stems from the NiBi₃ layer, this inevitably leads to a superconducting state that has a different environment close to the interfaces with Bi and Ni. We then speculate that the system studied here, the trilayer Ni/NiBi₃/Bi, in the limit of low Bi thickness, as we observed in the sample Ni(8nm)/Bi(20nm), could belong to the class of noncentrosymmetric superconductors. These materials experience inversion-breaking spin-orbit coupling effects enhancing the critical field.

To investigate the role of spin-orbit coupling in this system, we analyze the $B_{c2,\parallel}$ with the Werthamer-Helfand-Hohenberg (WHH) model. Three calculated theoretical curves and the experimental points are shown in Figs. 5d-f. This model incorporates both orbital and paramagnetic limiting mechanisms. The relative strength between these two effects is quantified by the Maki parameter [32], defined as $\alpha_M = \sqrt{2}B_{c2,\text{orb.}}(0)/B_P(0)$, where $B_{c2,\text{orb.}}$ and B_P are the orbital and paramagnetic limiting critical fields at zero temperature, respectively. For a single-band dirty-limit superconductor, the WHH model includes α_M and spin-orbit scattering (λ_{SO}). The overall upper critical field is obtained

from the equation below [33]:

$$\ln\left(\frac{1}{t}\right) = \sum_{v=-\infty}^{\infty} \left(\frac{1}{|2v+1|} - \left[|2v+1| + \frac{\bar{h}}{t} + \frac{(\alpha_M \bar{h}/t)^2}{|2v+1| + (\bar{h} + \lambda_{SO})/t} \right] \right),$$

where $\bar{h} = \left(\frac{4}{\pi^2} \frac{B_{c2}(t)}{|dB_{c2}(t)/dt|_{t=1}} \right)$.

Since the AGL model includes purely orbital effects, we considered $B_{c2,orb.}(0)$ as given by the slope obtained from fits with Eq. (2) near T_c , while $B_P(0) = 1.84T_c$ is established in the literature for BCS superconductors [34]. Thus, for Ni(8 nm)/Bi(20 nm), Ni(8 nm)/Bi(30 nm) and Ni(8 nm)/Bi(80 nm) samples we roughly estimate α_M as 2.80, 0.34 and 0.38, respectively.

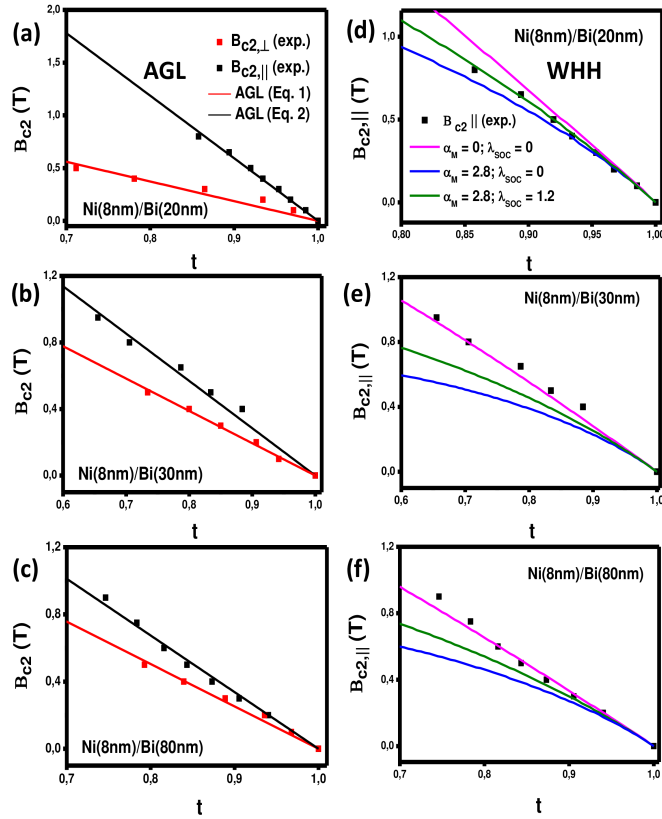


Figure 5: Upper critical field vs. temperature phase diagram analyzed within the scope of AGL theory in perpendicular (Eq. 1) and parallel 3D (Eq. 2) fields for Ni(8nm)/Bi(x) (a) $x = 20$ nm; (b) $x = 30$ nm and (c) $x = 80$ nm. Parallel upper critical field in function of reduced temperature within the scope of WHH model for Ni(8nm)/Bi(x) (d) $x = 20$ nm; (e) $x = 30$ nm and (f) $x = 80$ nm.

Fig. 5e,f presents the WHH fit for the thicker samples, with Bi layers of 30 and 80 nm. Notice that the best agreement to the experiments occurs for both parameters α_M and λ_{SO} equal to zero (magenta curve). This situation corresponds to $B_{c2,orb.}(0) \ll B_P(0)$ indicating a field-induced suppression of superconductivity due to orbital effects, as expected for ordinary type-II superconductors. The case of Ni(8nm)/Bi(20nm) sample

is more interesting, once the experimental points can be well described by introducing $\alpha_M = 2.8$ and $\lambda_{SO} = 1.2$, see Fig. 5d. It is essential to emphasize that our plots do not guarantee the existence of spin-orbit coupling. However, it can be considered as evidence that, at low thicknesses, the manifestation of spin-orbit effects can potentially account for the changes observed in the superconducting properties of the Ni/Bi system.

The origin of SC in the Ni/Bi bilayers is still a topic of debate. Whether it occurs at the Bi layer near the interface or whether it stems from bulk NiBi₃ formed at the interface remains a controversial subject. In this work, we find evidence in favor of the second hypothesis for thicker samples. In contrast, we point out the possibility of interesting effects occurring when very thin layers of NiBi₃ are formed at the bilayer interface. In this limit, the lack of inversion symmetry and the low thickness of the interfacial superconducting compound leads to a peculiar phenomenology such as that originated by an anti-symmetric spin-orbit coupling [35]. This adds to the claims favoring unconventional superconductivity reported so far in the Ni/Bi system [7, 12, 11, 13] and gives support to theoretical models as the one in Ref. [20]. Additionally, we notice that bulk NiBi₃ has been recently suggested as hosting a topological surface state [36], which might be a potential ingredient to be considered in the physics of thin Ni/Bi bilayers.

4 Conclusions

We investigated the structural properties and the temperature dependence of the upper critical field of polycrystalline Ni(8nm)/Bi(x) bilayers with $x = 10, 20, 30, 40, 60$ and 80 nm. XRD, RBS and VSM analysis indicated that the original bilayers actually form the trilayer structure Ni/NiBi₃/Bi. For samples with large Bi thickness, the structure becomes effectively NiBi₃/Bi. In the trilayer, the stray field due to the remaining layer of ferromagnetic Ni leads to a decrease in the critical temperature and to a broadening of the superconducting transition. The upper critical field was analyzed in the context of the AGL and WHH models. For larger Bi layer thicknesses, the coherence length is nearly isotropic ($\gamma = \xi_{\perp}(0)/\xi_{\parallel}(0) \approx 1$) and has values similar to that found for NiBi₃ single crystals. On the other hand, for low Bi thicknesses, an anisotropic behavior is observed ($\gamma = 0.32$). In the framework of the WHH model, thicker samples are described by a null Maki parameter and spin-orbit coupling. In the smallest Bi thickness sample, the Maki parameter ($\alpha_M = 2.8$) and the spin-orbit scattering ($\lambda_{SO} = 1.2$) are shown to be relevant to fully describe the temperature dependence of the upper critical field. Therefore, our results favor a thickness-dependent superconducting state in the Ni/Bi bilayer system.

Acknowledgments

The authors would like to acknowledge the funding agencies FAPERGS, CAPES and CNPq, in terms of the following grants: Pronex grant no. 16/0490-0 (Fapergs-CNPq)

References

- [1] F. Wilczek, “Majorana returns,” *Nature Physics*, vol. 5, no. 9, pp. 614–618, 2009.
- [2] C. Nayak, S. H. Simon, A. Stern, M. Freedman, and S. D. Sarma, “Non-abelian anyons and topological quantum computation,” *Reviews of Modern Physics*, vol. 80, no. 3, p. 1083, 2008.
- [3] S. Ran, C. Eckberg, Q.-P. Ding, Y. Furukawa, T. Metz, S. R. Saha, I.-L. Liu, M. Zic, H. Kim, J. Paglione *et al.*, “Nearly ferromagnetic spin-triplet superconductivity,” *Science*, vol. 365, no. 6454, pp. 684–687, 2019.
- [4] S. Saxena, P. Agarwal, K. Ahilan, F. Grosche, R. Haselwimmer, M. Steiner, E. Pugh, I. Walker, S. Julian, P. Monthoux *et al.*, “Superconductivity on the border of itinerant-electron ferromagnetism in UGe_2 ,” *Nature*, vol. 406, no. 6796, pp. 587–592, 2000.
- [5] D. Aoki, A. Huxley, E. Ressouche, D. Braithwaite, J. Flouquet, J.-P. Brison, E. Lhotel, and C. Paulsen, “Coexistence of superconductivity and ferromagnetism in $URhGe$,” *Nature*, vol. 413, no. 6856, pp. 613–616, 2001.
- [6] G. M. Luke, Y. Fudamoto, K. Kojima, M. Larkin, J. Merrin, B. Nachumi, Y. Uemura, Y. Maeno, Z. Mao, Y. Mori *et al.*, “Time-reversal symmetry-breaking superconductivity in Sr_2RuO_4 ,” *Nature*, vol. 394, no. 6693, pp. 558–561, 1998.
- [7] X. Gong, M. Kargarian, A. Stern, D. Yue, H. Zhou, X. Jin, V. M. Galitski, V. M. Yakovenko, and J. Xia, “Time-reversal symmetry-breaking superconductivity in epitaxial bismuth/nickel bilayers,” *Science advances*, vol. 3, no. 3, p. e1602579, 2017.
- [8] O. Prakash, A. Kumar, A. Thamizhavel, and S. Ramakrishnan, “Evidence for bulk superconductivity in pure bismuth single crystals at ambient pressure,” *Science*, vol. 355, no. 6320, pp. 52–55, 2017.
- [9] J. Moodera and R. Meservey, “Superconducting phases of Bi and Ga induced by deposition on a Ni sublayer,” *Physical Review B*, vol. 42, no. 1, p. 179, 1990.
- [10] P. LeClair, J. Moodera, J. Philip, and D. Heiman, “Coexistence of ferromagnetism and superconductivity in Ni/Bi bilayers,” *Physical review letters*, vol. 94, no. 3, p. 037006, 2005.

- [11] P. Chauhan, F. Mahmood, D. Yue, P.-C. Xu, X. Jin, and N. Armitage, “Nodeless bulk superconductivity in the time-reversal symmetry breaking bi/ni bilayer system,” *Physical review letters*, vol. 122, no. 1, p. 017002, 2019.
- [12] X.-X. Gong, H.-X. Zhou, P.-C. Xu, D. Yue, K. Zhu, X.-F. Jin, H. Tian, G.-J. Zhao, and T.-Y. Chen, “Possible p-wave superconductivity in epitaxial bi/ni bilayers,” *Chinese Physics Letters*, vol. 32, no. 6, p. 067402, 2015.
- [13] J. Wang, X. Gong, G. Yang, Z. Lyu, Y. Pang, G. Liu, Z. Ji, J. Fan, X. Jing, C. Yang *et al.*, “Anomalous magnetic moments as evidence of chiral superconductivity in a bi/ni bilayer,” *Physical Review B*, vol. 96, no. 5, p. 054519, 2017.
- [14] G. Zhao, X. Gong, P. Xu, B. Li, Z. Huang, X. Jin, X.-D. Zhu, and T. Chen, “Singlet superconductivity in a single-crystal nibi₃ superconductor,” *Superconductor Science and Technology*, vol. 31, no. 12, p. 125005, 2018.
- [15] X. Zhu, H. Lei, C. Petrovic, Y. Zhang *et al.*, “Surface-induced magnetic fluctuations in a single-crystal nibi₃ superconductor,” *Physical Review B*, vol. 86, no. 2, p. 024527, 2012.
- [16] Y. Fujimori, S.-i. Kan, B. Shinozaki, and T. Kawaguti, “Superconducting and normal state properties of nibi₃,” *Journal of the Physical Society of Japan*, vol. 69, no. 9, pp. 3017–3026, 2000.
- [17] V. Siva, K. Senapati, B. Satpati, S. Prusty, D. Avasthi, D. Kanjilal, and P. K. Sahoo, “Spontaneous formation of superconducting nibi₃ phase in ni-bi bilayer films,” *Journal of Applied Physics*, vol. 117, no. 8, p. 083902, 2015.
- [18] M. Vaughan, N. Satchell, M. Ali, C. J. Kinane, G. B. Stenning, S. Langridge, and G. Burnell, “Origin of superconductivity at nickel-bismuth interfaces,” *Physical Review Research*, vol. 2, no. 1, p. 013270, 2020.
- [19] L. Liu, Y. Xing, I. Merino, H. Micklitz, D. Franceschini, E. Baggio-Saitovitch, D. Bell, and I. Solórzano, “Superconductivity in bi/ni bilayer system: Clear role of superconducting phases found at bi/ni interface,” *Physical Review Materials*, vol. 2, no. 1, p. 014601, 2018.
- [20] S.-P. Chao, “Superconductivity in a bi/ni bilayer,” *Physical Review B*, vol. 99, no. 6, p. 064504, 2019.
- [21] J. Kumar, A. Kumar, A. Vajpayee, B. Gahtori, D. Sharma, P. Ahluwalia, S. Auluck, and V. Awana, “Physical property and electronic structure characterization of bulk superconducting bi₃ni,” *Superconductor Science and Technology*, vol. 24, no. 8, p. 085002, 2011.

- [22] B. Silva, R. Luccas, N. Nemes, J. Hanko, M. Osorio, P. Kulkarni, F. Mompean, M. García-Hernández, M. Ramos, S. Vieira *et al.*, “Superconductivity and magnetism on flux-grown single crystals of ni₃,” *Physical Review B*, vol. 88, no. 18, p. 184508, 2013.
- [23] L. Liebermann, J. Clinton, D. Edwards, and J. Mathon, ““ dead” layers in ferromagnetic transition metals,” *Physical Review Letters*, vol. 25, no. 4, p. 232, 1970.
- [24] S. Xiao, D. Wei, and X. Jin, “Bi (111) thin film with insulating interior but metallic surfaces,” *Physical review letters*, vol. 109, no. 16, p. 166805, 2012.
- [25] H. Zhou, X. Gong, and X. Jin, “Magnetic properties of superconducting bi/ni bilayers,” *Journal of Magnetism and Magnetic Materials*, vol. 422, pp. 73–76, 2017.
- [26] T. Schneider and J.-P. Locquet, “Dimensional crossover and finite size effects in superconducting films,” *Physica C: Superconductivity*, vol. 179, no. 1-3, pp. 125–130, 1991.
- [27] M. Tinkham, *Introduction to superconductivity*. Courier Corporation, 2004.
- [28] N. Pinto, S. J. Rezvani, A. Perali, L. Flammia, M. V. Milošević, M. Fretto, C. Casiago, and N. De Leo, “Dimensional crossover and incipient quantum size effects in superconducting niobium nanofilms,” *Scientific reports*, vol. 8, no. 1, p. 4710, 2018.
- [29] F. Harper and M. Tinkham, “The mixed state in superconducting thin films,” *Physical Review*, vol. 172, no. 2, p. 441, 1968.
- [30] C. S. Chun, G.-G. Zheng, J. L. Vincent, and I. K. Schuller, “Dimensional crossover in superlattice superconductors,” *Physical Review B*, vol. 29, no. 9, p. 4915, 1984.
- [31] R. A. Klemm, M. Beasley, and A. Luther, “The upper critical field of layered superconductors,” *Journal of Low Temperature Physics*, vol. 16, pp. 607–613, 1974.
- [32] K. Maki, “Effect of pauli paramagnetism on magnetic properties of high-field superconductors,” *Physical Review*, vol. 148, no. 1, p. 362, 1966.
- [33] N. Werthamer, E. Helfand, and P. Hohenberg, “Temperature and purity dependence of the superconducting critical field, h_c2 . iii. electron spin and spin-orbit effects,” *Physical Review*, vol. 147, no. 1, p. 295, 1966.
- [34] A. M. Clogston, “Upper limit for the critical field in hard superconductors,” *Physical Review Letters*, vol. 9, no. 6, p. 266, 1962.
- [35] M. Smidman, M. Salamon, H. Yuan, and D. Agterberg, “Superconductivity and spin-orbit coupling in non-centrosymmetric materials: a review,” *Reports on Progress in Physics*, vol. 80, no. 3, p. 036501, 2017.

- [36] C. Adriano, K. Lee, Y. Kushnirenko, B. Schruck, K. R. Pakuszewski, L.-L. Wang, S. L. Bud'ko, P. C. Canfield, and A. Kaminski, "Bulk and surface electronic structure of NiBi_3 ," *Physical Review B*, vol. 107, no. 16, p. 165107, 2023.